ACADEMIC PRESS

Available online at www.sciencedirect.com

SCIENCE DIRECT®

Journal of Sound and Vibration 267 (2003) 67–86

JOURNAL OF SOUND AND VIBRATION

www.elsevier.com/locate/jsvi

An elastodynamic solution of finite long orthotropic hollow cylinder under torsion impact

X. Wang*, X.H. Xia, W.H. Hao

Department of Engineering Mechanics, The School of Civil Engineering and Mechanics, Shanghai Jiaotong University, Shanghai 200240, People's Republic of China

Received 19 January 2001; accepted 7 October 2002

Abstract

The paper presents an analytical method to solve the elastodynamic problem of a finite-length orthotropic hollow cylinder subjected to a torsion impact often occurring in engineering fields. The elastodynamic solution is composed of a quasi-static solution of homogeneous equation satisfied with the non-homogeneous boundary condition and a dynamic solution of non-homogeneous equation satisfied with homogeneous boundary condition. The quasi-static solution can be obtained by directly solving the quasi-static equation satisfied with the non-homogeneous boundary condition. The solution of a non-homogeneous dynamic equation is obtained by means of a finite Hankel transform to a radial variable r, Laplace transform to a time variable t and finite Fourier transform to an axial variable z. Thus, the elastodynamic solution of the finite length of an orthotropic hollow cylinder subjected to a torsion impact is obtained. On the other hand, a dynamic finite element for the same problem is also carried out by applying the ANSYS finite-element analysis system. Comparing the theoretical solution with finite-element solution, it can be found that two kinds of results obtained by making use of two different solving methods are suitably approached. Therefore, it is further concluded that the methods and computing processes of the theoretical solution are effective and accurate.

1. Introduction

It is known that the dynamic response of a hollow cylinder under torsion impact became an attentive engineering problem for a long time in many cases, such as, in the course of mechanical drilling, geologic prospecting, drilling, petroleum drilling and automatic fastening of steel structure's fastening bolts. It is possible to induce various actions of torsion impact, to a hollow cylinder, geology, rock, and so on, including isotropic and anisotropic materials.

*Corresponding author.
E-mail address: xwang@mail.sjtu.edu.cn (X. Wang).

0022-460X/03/$ - see front matter © 2002 Elsevier Ltd. All rights reserved.
doi:10.1016/S0022-460X(02)01413-X

Solving the problem of elastic wave propagation in a hollow cylinder or a hollow sphere by using the theory of elastodynamics has been done in many works. But it was always limited to the situation of radial impact [1–6]. The research of the problem of solving a hollow cylinder subjected to torsion impact by means of the theory of elastodynamics is very few. Ref. [7] studied the response histories and distribution of a semi-infinite and infinite elastic body under a torsion force with time and uniform distribution along one of the cylinders. Ref. [8] studied the response histories of torsion stress wave in a cylindrical waveguide tube with longitudinal section periodic changing by using the theory of elasticity and experiment. Ref. [9] presents the theoretical solution of elastodynamics about an infinite length hollow cylinder subjected to torsion impact. But through analyzing, it was found that it does not satisfy the given boundary condition.

This paper sets up the corresponding dynamic model regarding the problem of finite length of an orthotropic hollow cylinder subjected to torsion impact, based on the mixed boundary condition. The elastodynamic solution is composed of a quasi-static solution satisfied with a non-homogeneous boundary condition and a dynamic solution satisfied with homogeneous boundary condition. The quasi-static solution is obtained by means of a direct integral for the quasi-static equation with non-homogeneous boundary condition. The solution of a non-homogeneous dynamic equation with the corresponding homogeneous boundary condition is obtained by making use of a finite Hankel transform to a radial variable r, Laplace transform to time variable t and finite Fourier transform to axial variable z.

In the example calculating, the responding histories and distributions of shear stress in a finite-length orthotropic hollow cylinder subjected to torsion impact load have been obtained. By analyzing the result of computing, it is seen that the solution obtained in the paper appears in the wave's properties and there exists a strong discontinuity effect at the wavefront of the shear stress wave.

In order to further prove that the method and computing process of the theoretical solution are effective and accurate, a dynamic finite-element solution for the same problem is also carried out by using the ANSYS finite-element analysis system. Comparing the results of the theoretical solution with the finite-element solution, it can be found that the two kinds of results obtained by making use of two different methods are approached very well.

2. Solving method of orthotropic hollow cylinder under torsion impact

The structure of a finite-length orthotropic hollow cylinder with the outer boundary fixed and inter-wall subjected to a torsion impact load $A(z,t)$ is shown in Fig. 1.

In a cylindrical co-ordinate system, the generalized Hooke's law of an orthotropic hollow cylinder is given by

$$\begin{Bmatrix} \sigma_r \\ \sigma_\theta \\ \sigma_z \\ \tau_{\theta z} \\ \tau_{rz} \\ \tau_{r\theta} \end{Bmatrix} = \begin{bmatrix} C_{11} & C_{12} & C_{13} & 0 & 0 & 0 \\ C_{12} & C_{22} & C_{23} & 0 & 0 & 0 \\ C_{13} & C_{23} & C_{33} & 0 & 0 & 0 \\ 0 & 0 & 0 & C_{44} & 0 & 0 \\ 0 & 0 & 0 & 0 & C_{55} & 0 \\ 0 & 0 & 0 & 0 & 0 & C_{66} \end{bmatrix} 0 \begin{Bmatrix} \varepsilon_r \\ \varepsilon_\theta \\ \varepsilon_z \\ \gamma_{\theta z} \\ \gamma_{rz} \\ \gamma_{r\theta} \end{Bmatrix}. \tag{1}$$

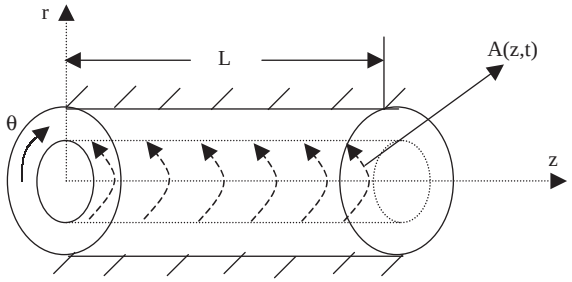

Fig. 1. The structural model.

Considering the forms of geometry and load of the structure shown in Fig. 1, the strains and displacements of the finite length of an orthotropic hollow cylinder subjected to torsion impact are independent of θ and $U_r = U_z = 0$. The corresponding geometrical equation is expressed as

$$\begin{gathered}\varepsilon_r = \varepsilon_\theta = \varepsilon_z = \gamma_{rz} = 0,\\ \gamma_{\theta z} = \frac{\partial U_\theta}{\partial z}, \quad \gamma_{r\theta} = \frac{\partial U_\theta}{\partial r} - \frac{U_\theta}{r}.\end{gathered} \tag{2}$$

Substituting Eq. (2) into Eq. (1) yields

$$\tau_{\theta z} = C_{44}\frac{\partial U_\theta}{\partial z}, \quad \tau_{r\theta} = C_{66}\left(\frac{\partial U_\theta}{\partial r} - \frac{U_\theta}{r}\right). \tag{3}$$

In the cylinder co-ordinate system, dynamic equilibrium equations are written as

$$\begin{gathered}\frac{\partial \sigma_r}{\partial r} + \frac{\sigma_r - \sigma_\theta}{r} + \frac{\partial \tau_{zr}}{\partial z} = \rho\frac{\partial^2 U_r}{\partial t^2},\\ \frac{\partial \tau_{\theta r}}{\partial r} + \frac{\partial \tau_{\theta z}}{\partial z} + \frac{2\tau_{r\theta}}{r} = \rho\frac{\partial^2 U_\theta}{\partial t^2},\\ \frac{\partial \tau_{rz}}{\partial r} + \frac{\partial \sigma_z}{\partial z} + \frac{\tau_{rz}}{r} = \rho\frac{\partial^2 U_z}{\partial t^2}.\end{gathered} \tag{4}$$

Substituting Eq. (3) into Eq. (4), the elastodynamic equilibrium equation of the finite length of an orthotropic hollow cylinder subjected to torsion impact is simplified to

$$\begin{gathered}\frac{\partial^2 U_\theta(r,z,t)}{\partial r^2} + \frac{1}{r}\frac{\partial U_\theta(r,z,t)}{\partial r} - \frac{U_\theta(r,z,t)}{r^2} + R^2\frac{\partial^2 U_\theta(r,z,t)}{\partial z^2} = \frac{1}{C_\tau^2}\frac{\partial^2 U_\theta(r,z,t)}{\partial t^2},\\ a \leqslant r \leqslant b,\ 0 \leqslant z \leqslant L,\ t \geqslant 0,\end{gathered} \tag{5}$$

where $R^2 = C_{44}/C_{66}$ and $C_\tau^2 = C_{66}/\rho$.

The boundary condition and initial condition are, respectively, given as

$$\tau_{r\theta}(r,z,t)_{r=a} = C_{66}\left(\frac{\partial U_\theta(r,z,t)}{\partial r} - \frac{U_\theta(r,z,t)}{r}\right) = A(z,t), \tag{6a}$$

$$U_\theta(r,z,t)_{r=b} = 0, \tag{6b}$$

$$\tau_{\theta z}(r,z,t)_{z=0} = C_{44}\frac{\partial U_\theta(r,0,t)}{\partial z} = 0, \tag{6c}$$

$$\tau_{\theta z}(r,z,t)_{z=L} = C_{44}\frac{\partial U_\theta(r,L,t)}{\partial z} = 0, \tag{6d}$$

$$U_\theta(r,z,t)_{t=0} = U_0(r,z), \tag{6e}$$

$$\frac{\partial U_\theta(r,z,t)}{\partial t}|_{t=0} = V_{\vartheta 0}(r,z). \tag{6f}$$

Suppose the solution of Eq. (5) is

$$U_\theta(r,z,t) = U_{\theta s}(r,z,t) + U_{\theta d}(r,z,t), \tag{7}$$

where $U_{\theta s}(r,z,t)$ represents the solution of a quasi-static equation satisfied with the non-homogeneous boundary condition and $U_{\theta d}(r,z,t)$ represents the solution of a dynamic equation satisfied with the homogeneous boundary condition. The quasi-static equation is expressed as

$$\frac{\partial^2 U_{\theta s}(r,z,t)}{\partial r^2} + \frac{1}{r}\frac{\partial U_{\theta s}(r,z,t)}{\partial r} - \frac{U_{\theta s}(r,z,t)}{r^2} = 0 \tag{8a}$$

and $U_{\theta s}(r,z,t)$ satisfied with the following non-homogeneous boundary condition:

$$C_{66}\left(\frac{\partial U_{\theta s}(r,z,t)}{\partial r} - \frac{U_{\theta s}(r,z,t)}{r}\right)_{r=a} = A(z,t),$$
$$U_{\theta s}(r,z,t)_{r=b} = 0. \tag{8b}$$

The solution of differential equation (8) can be given by

$$U_{\theta s}(r,z,t) = C_1 r + C_2 r^{-1}. \tag{9}$$

Utilizing the non-homogeneous boundary condition (8b), the quasi-static solution $U_{\theta s}(r,z,t)$ is written as

$$U_{\theta s}(r,z,t) = \frac{a^2}{2C_{66}}\left(\frac{r}{b^2} - \frac{1}{r}\right)A(z,t). \tag{10}$$

Substituting Eq. (7) into Eq. (5) and utilizing Eqs. (6), the non-homogeneous dynamic equation which the dynamic solution $U_{\theta d}(r,z,t)$ should satisfy, the corresponding homogeneous boundary condition and initial condition are, respectively, represented as

$$\frac{\partial^2 U_{\theta d}(r,z,t)}{\partial r^2} + \frac{1}{r}\frac{\partial U_{\theta d}(r,z,t)}{\partial r} - \frac{U_{\theta d}(r,z,t)}{r^2}$$
$$= \frac{1}{C_\tau^2}\left(\frac{\partial^2 U_{\theta s}(r,z,t)}{\partial t^2} + \frac{\partial^2 U_{\theta d}(r,z,t)}{\partial t^2}\right) - R^2\left(\frac{\partial^2 U_{\theta s}(r,z,t)}{\partial z^2} + \frac{\partial^2 U_{\theta d}(r,z,t)}{\partial z^2}\right), \tag{11a}$$

$$\left(\frac{\partial U_{\theta d}(r,z,t)}{\partial r} - \frac{U_{\theta d}(r,z,t)}{r}\right)|_{r=a} = 0, \tag{11b}$$

$$U_{\theta d}(r,z,t)_{r=b} = 0, \tag{11c}$$

$$U_{\theta d}(r,z,0) = U_{\theta 0}(r,z) - U_{\theta s0}(r,z,0), \tag{11d}$$

$$\frac{\partial U_{\theta d}(r,z,0)}{\partial t} = V_{\theta 0}(r,z) - \frac{\partial U_{\theta s}(r,z,0)}{\partial t} = V_{\theta 0}(r,z) - V_{\theta s0}(r,z). \tag{11e}$$

In non-homogeneous dynamic equation (11a), $U_{\theta s}(r,z,t)$ is the known quasi-static solution shown in formula (10).

Defining finite Hanker transform [10] to a radial variable r of $U_{\theta d}(r,z,t)$ in a non-homogeneous dynamic equation as

$$\mathrm{H}[U_{\theta d}(r,z,t)] = \bar{U}_{\theta d}(\xi_i,z,t) = \int_a^b U_{\theta d}(r,z,t) r C_1(\xi_i r)\,\mathrm{d}r, \tag{12}$$

its inverse transform is

$$U_{\theta d}(r,z,t) = \sum_{\xi_i} \frac{\bar{U}_{\theta d}(\xi_i,z,t)}{F(\xi_i)} C_1(\xi_i r), \tag{13}$$

where

$$C_1(\xi_i r) = \mathrm{J}_1(\xi_i r)\mathrm{Y}_1(\xi_i b) - \mathrm{J}_1(\xi_i b)\mathrm{Y}_1(\xi_i r) \tag{14}$$

and

$$F(\xi_i) = \int_a^b r C_1^2(\xi_i r)\,\mathrm{d}r. \tag{15}$$

ξ_i $(i = 1,2,3,\ldots)$ are positive eigenroots which should satisfy the following characteristic equation:

$$\mathrm{Y}_1(\xi_i b)[\xi_i \mathrm{J}_1(\xi_i a) - \frac{1}{a}\mathrm{J}_1(\xi_i a)] - \mathrm{J}_1(\xi_i b)[\xi_i \mathrm{Y}_1(\xi_i a) - \frac{1}{a}\mathrm{Y}_1(\xi_i a)] = 0. \tag{16}$$

Applying a finite Hankel transform on the radial variable r to the two sides of non-homogeneous dynamic equation (10a), we have

$$\begin{aligned}&\mathrm{H}\left[\frac{\partial^2 U_{\theta d}(r,z,t)}{\partial r^2} + \frac{1}{r}\frac{\partial U_{\theta d}(r,z,t)}{\partial r} - \frac{U_{\theta d}(r,z,t)}{r^2}\right]\\ &\quad = \frac{1}{C_\tau^2}\mathrm{H}\left[\frac{\partial^2 U_{\theta s}(r,z,t)}{\partial t^2} + \frac{\partial^2 U_{\theta d}(r,z,t)}{\partial t^2}\right] - R^2\mathrm{H}\left[\frac{\partial^2 U_{\theta s}(r,z,t)}{\partial z^2} + \frac{\partial^2 U_{\theta d}(r,z,t)}{\partial z^2}\right].\end{aligned} \tag{17}$$

Utilizing boundary condition (11b,c), the finite Hankel transform of the left side of Eq. (17) can be shown as

$$\mathrm{H}\left[\frac{\partial^2 U_{\theta d}(r,z,t)}{\partial r^2} + \frac{1}{r}\frac{\partial U_{\theta d}(r,z,t)}{\partial r} - \frac{U_{\theta d}(r,z,t)}{r^2}\right] = -\xi_i^2 \bar{U}_{\theta d}(\xi_i,z,t) \tag{18}$$

and the finite Hankel transform of the right side of Eq. (17) can be shown as

$$\begin{aligned}&\frac{1}{C_\tau^2}\mathrm{H}\left[\frac{\partial^2 U_{\theta s}(r,z,t)}{\partial t^2} + \frac{\partial^2 U_{\theta d}(r,z,t)}{\partial t^2}\right] - R^2\mathrm{H}\left[\frac{\partial^2 U_{\theta s}(r,z,t)}{\partial z^2} + \frac{\partial^2 U_{\theta d}(r,z,t)}{\partial z^2}\right]\\ &\quad = \frac{1}{C_\tau^2}\left[\frac{\partial^2 \bar{U}_{\theta s}(\xi_i,z,t)}{\partial t^2} + \frac{\partial^2 \bar{U}_{\theta d}(\xi_i,z,t)}{\partial t^2}\right] - R^2\left[\frac{\partial^2 \bar{U}_{\theta s}(\xi_i,z,t)}{\partial z^2} + \frac{\partial^2 \bar{U}_{\theta d}(\xi_i,z,t)}{\partial z^2}\right].\end{aligned} \tag{19}$$

Substituting Eqs. (18) and (19) into Eq. (17) yields

$$-\xi_i^2 \bar{U}_{\theta d}(\xi_i, z, t) = \frac{1}{C_\tau^2}\left[\frac{\partial^2 \bar{U}_{\theta d}(\xi_i, z, t)}{\partial t^2} + \frac{\partial^2 \bar{U}_{\theta d}(\xi_i, z, t)}{\partial t^2}\right] - R^2\left[\frac{\partial^2 \bar{U}_{\theta d}(\xi_i, z, t)}{\partial z^2} + \frac{\partial^2 \bar{U}_{\theta d}(\xi_i, z, t)}{\partial z^2}\right]. \tag{20}$$

In order to solve $\bar{U}_{\theta d}(\xi_i, z, t)$, applying Laplace transform to the axial variable z in Eq. (20), we have

$$-\xi_i^2 L[\bar{U}_{\theta d}(\xi_i, z, t)] = \frac{1}{C_\tau^2} L\left[\frac{\partial^2 \bar{U}_{\theta s}(\xi_i, z, t)}{\partial t^2} + \frac{\partial^2 \bar{U}_{\theta d}(\xi_i, z, t)}{\partial t^2}\right] - R^2 L\left[\frac{\partial^2 \bar{U}_{\theta s}(\xi_i, z, t)}{\partial z^2} + \frac{\partial^2 \bar{U}_{\theta d}(\xi_i, z, t)}{\partial z^2}\right]. \tag{21}$$

The left side of Eq. (21) can be written as

$$-\xi_i^2 L[\bar{U}_{\theta d}(\xi_i, z, t)] = -\xi_i^2[\bar{U}^*_{\theta d}(\xi_i, z, p)] \tag{22a}$$

and the right side of Eq. (21) can be written as

$$\begin{aligned}&\frac{1}{C_\tau^2} L\left[\frac{\partial^2 \bar{U}_{\theta s}(\xi_i, z, t)}{\partial t^2} + \frac{\partial^2 \bar{U}_{\theta d}(\xi_i, z, t)}{\partial t^2}\right] - R^2 L\left[\frac{\partial^2 \bar{U}_{\theta s}(\xi_i, z, t)}{\partial z^2} + \frac{\partial^2 \bar{U}_{\theta d}(\xi_i, z, t)}{\partial z^2}\right] \\ &= \frac{1}{C_\tau^2}\left\{p^2\left[\frac{\partial^2 \bar{U}^*_{\theta s}(\xi_i, z, p)}{\partial t^2} + \frac{\partial^2 \bar{U}^*_{\theta d}(\xi_i, z, p)}{\partial t^2}\right] - p\,\bar{U}_{\theta d}(\xi_i, z) - \bar{V}_{\theta d}(\xi_i, z)\right\} \\ &\quad - R^2\left[\frac{\partial^2 \bar{U}^*_{\theta s}(\xi_i, z, p)}{\partial z^2} + \frac{\partial^2 \bar{U}^*_{\theta d}(\xi_i, z, p)}{\partial z^2}\right].\end{aligned} \tag{22b}$$

Thus, Laplace transform of Eq. (21) is represented as

$$\begin{aligned}-\xi_i^2[\bar{U}^*_{\theta d}(\xi_i, z, p)] = &\frac{1}{C_\tau^2}\{p^2[\bar{U}^*_{\theta s}(\xi_i, z, p) + \bar{U}^*_{\theta d}(\xi_i, z, p)] - p\,\bar{U}_0(\xi_i, z) - \bar{V}_0(\xi_i, z)\} \\ &- R^2\left[\frac{\partial^2 \bar{U}^*_{\theta s}(\xi_i, z, p)}{\partial z^2} + \frac{\partial^2 \bar{U}^*_{\theta d}(\xi_i, z, p)}{\partial z^2}\right],\end{aligned} \tag{23a}$$

where

$$\bar{U}_{\theta 0}(\xi_i, z) = \int_a^b U_{\theta 0}(r, z) r C_1(\xi_i r)\,\mathrm{d}r, \tag{23b}$$

$$\bar{V}_{\theta 0}(\xi_i, z) = \int_a^b V_{\theta 0}(r, z) r C_1(\xi_i r)\mathrm{d}r. \tag{23c}$$

Define, respectively, finite Fourier transform and its inverse transform as

$$\Phi[f(x)] = F(n) = \int_0^L f(x)\cos\frac{n\pi x}{L}\,\mathrm{d}x, \quad n = 0, 1, 2, 3\ldots, \tag{24a}$$

$$\Phi^{-1}[F(n)] = f(x) = \frac{1}{L}F(0) + \frac{2}{L}\sum_{n=1}^{\infty} F(n)\cos\frac{n\pi x}{L}. \tag{24b}$$

To make $U_{\theta s}(r, z, t)$ and $U_{\theta d}(r, z, t)$ satisfy boundary condition (6c,d) when $z = 0$ and L, the finite Fourier transform to them is represented as

$$U_{\theta s}(r, z, t) = \sum_{n=0}^{\infty} \tilde{U}_{\theta s}(r, n, t)\cos\frac{n\pi z}{L}, \tag{25a}$$

$$U_{\theta d}(r, z, t) = \sum_{n=0}^{\infty} \tilde{U}_{\theta d}(r, n, t)\cos\frac{n\pi z}{L}. \tag{25b}$$

Substituting Eqs. (25) and (24) into Eq. (23a) yields

$$\begin{aligned} -\xi_i^2\,\tilde{\tilde{U}}^*_{\theta d}(\xi_i, n, p) = {} & \frac{1}{C_\tau^2}[p^2\,\tilde{\tilde{U}}^*_{\theta s}(\xi_i, n, p) + p^2\,\tilde{\tilde{U}}^*_{\theta d}(\xi_i, n, p) - p\,\tilde{\tilde{U}}_{\theta 0}(\xi_i, n) - \tilde{\tilde{V}}_{\theta 0}(\xi_i, n)] \\ & + \frac{n^2\pi^2 R^2}{L^2}[\tilde{\tilde{U}}^*_{\theta s}(\xi_i, n, p) + \tilde{\tilde{U}}^*_{\theta d}(\xi_i, n, p)], \quad (n = 0, 1, 2, 3, \ldots), \end{aligned} \tag{26}$$

where

$$\begin{aligned} &\tilde{\tilde{U}}^*_{\theta d}(\xi_i, 0, p) = \frac{1}{L}\int_0^L \tilde{\tilde{U}}^*_{\theta d}(\xi_i, z, p)\,\mathrm{d}z, \\ &\tilde{\tilde{U}}^*_{\theta d}(\xi_i, n, p) = \frac{2}{L}\int_0^L \tilde{\tilde{U}}^*_{\theta d}(\xi_i, z, p)\,\mathrm{d}z, \\ &\tilde{\tilde{U}}^*_{\theta d}(\xi_i, 0, p) = \frac{1}{L}\int_0^L \tilde{\tilde{U}}^*_{\theta s}(\xi_i, z, p)\,\mathrm{d}z, \\ &\tilde{\tilde{U}}^*_{\theta d}(\xi_i, n, p) = \frac{2}{L}\int_0^L \tilde{\tilde{U}}^*_{\theta s}(\xi_i, z, p)\,\mathrm{d}z, \\ &\tilde{\tilde{U}}_{\theta 0}(\xi_i, 0) = \frac{1}{L}\int_0^L \bar{U}_{\theta 0}(\xi_i, z)\,\mathrm{d}z, \quad \tilde{\tilde{U}}_{\theta 0}(\xi_i, n) = \frac{2}{L}\int_0^L \bar{U}_{\theta 0}(\xi_i, z)\,\mathrm{d}z, \\ &\tilde{\tilde{V}}_{\theta 0}(\xi_i, 0) = \frac{1}{L}\int_0^L \bar{V}_{\theta 0}(\xi_i, z)\,\mathrm{d}z, \quad \tilde{\tilde{V}}_{\theta 0}(\xi_i, n) = \frac{2}{L}\int_0^L \bar{V}_{\theta 0}(\xi_i, z)\,\mathrm{d}z. \end{aligned} \tag{27}$$

To make Laplace inverse transform of Eq. (26) be easier, Eq. (26) is simplified to

$$\begin{aligned} \tilde{\tilde{U}}^*_{\theta d}(\xi_i, n, p) = {} & -\tilde{\tilde{U}}^*_{\theta s}(\xi_i, n, p) + \frac{\xi_i^2 C_\tau^2}{p^2 + X^2}\,\tilde{\tilde{U}}^*_{\theta s}(\xi_i, n, p) - \frac{p}{p^2 + X^2}\,\tilde{\tilde{U}}_{\theta 0}(\xi_i, n) \\ & - \frac{1}{p^2 + X^2}\,\tilde{\tilde{V}}_{\theta 0}(\xi_i, n), \end{aligned} \tag{28a}$$

where

$$X^2 = \xi_i^2 C_\tau^2 + \frac{n^2\pi^2 R^2 C_\tau^2}{L^2}. \tag{28b}$$

Laplace inverse transform to Eq. (26) gives

$$\tilde{\tilde{U}}_{\theta d}(\xi_i, n, t) = -\tilde{\tilde{U}}_{\theta s}(\xi_i, n, t) + \frac{\xi_i^2 C_\tau^2}{X} \sin Xt * \tilde{\tilde{U}}_{\theta s}(\xi_i, n, t) - \tilde{\tilde{U}}_{\theta 0}(\xi_i, n) \cos Xt - \frac{\sin Xt}{X} \tilde{\tilde{V}}_{\theta 0}(\xi_i, n), \tag{29a}$$

where

$$\sin Xt * \tilde{\tilde{U}}_{\theta s}(\xi_i, n, t) = \int_0^t \sin X(t-\tau) \tilde{\tilde{U}}_{\theta s}(\xi_i, n, \tau)\, \mathrm{d}\tau. \tag{29b}$$

For $n = 0$, Eq. (29a) can be written as

$$\tilde{\tilde{U}}_{\theta d}(\xi_i, 0, t) = -\tilde{\tilde{U}}_{\theta s}(\xi_i, 0, t) + \xi_i C_\tau \sin(\xi_i C_\tau t) * \tilde{\tilde{U}}_{\theta s}(\xi_i, 0, t) - \tilde{\tilde{U}}_{\theta 0}(\xi_i, 0) \cos(\xi_i C_\tau t) - \frac{\sin(\xi_i C_\tau t)}{\xi_i C_\tau} \tilde{\tilde{V}}_{\theta 0}(\xi_i, 0). \tag{30}$$

Substituting Eq. (29) into Eq. (25) and applying Fourier inverse transform of $\tilde{\tilde{U}}_{\theta d}(\xi_i, n, t)$ yields

$$\bar{U}_{\theta d}(\xi_i, z, t) = \sum_{n=0}^{\infty} \tilde{\tilde{U}}_{\theta d}(\xi_i, n, t) \cos \frac{n\pi z}{L}. \tag{31}$$

Substituting Eq. (31) into Eq. (13), the dynamic solution $U_{\theta d}(r, z, t)$ of non-homogeneous dynamic equation (11) satisfied with the homogeneous boundary condition is represented as

$$U_{\theta d}(r, z, t) = \sum_{\xi_i}^{\infty} \frac{\sum_{n=0}^{\infty} \tilde{\tilde{U}}_{\theta d}(\xi_i, n, t) \cos \dfrac{n\pi z}{L}}{F(\xi_i)} C_1(\xi_i r). \tag{32}$$

Substituting quasi-static solution (10) $U_{\theta s}(r, z, t)$ and dynamic solution (32) $U_{\theta d}(r, z, t)$ into Eq. (7), the elastodynamic solution of the finite length of an orthotropic hollow cylinder subjected to torsion impact is represented as

$$U_\theta(r, z, t) = \frac{a^2}{2C_{66}} \left(\frac{r}{b^2} - \frac{1}{r} \right) \sum_{n=0}^{\infty} \tilde{A}(n, t) \cos \frac{n\pi z}{L} + \sum_{\xi_i}^{\infty} \frac{\sum_{n=0}^{\infty} \tilde{\tilde{U}}_{\theta d}(\xi_i, n, t) \cos \dfrac{n\pi z}{L}}{F(\xi_i)} C_1(\xi_i r), \tag{33a}$$

where

$$\bar{A}(0, t) = \frac{1}{L} \int_0^L A(z, t)\, \mathrm{d}z,$$

$$\bar{A}(n, t) = \frac{2}{L} \int_0^L A(z, t) \cos \frac{n\pi z}{L}\, \mathrm{d}z \quad (n = 1, 2, 3, \ldots). \tag{33b}$$

Substituting elastodynamic solution (33) into Eq. (3), dynamic shear stresses $\tau_{r\theta}$ and $\tau_{\theta z}$ in the finite length of an orthotropic hollow cylinder are given by

$$\tau_{r\theta} = \frac{a^2}{r^2}\sum_{n=0} A(n,t)\cos\frac{n\pi z}{L} + C_{66}\sum_{\xi_i}\frac{\sum_{n=0}\tilde{U}_{\theta d}(\xi_i,n,t)\cos\dfrac{n\pi z}{L}}{F(\xi_i)}\left[\frac{\mathrm{d}C_1(\xi_i r)}{\mathrm{d}r} - \frac{C_1(\xi_i r)}{r}\right],$$

$$\tau_{\theta z} = \frac{a^2 C_{44}}{2C_{66}}\left(\frac{r}{b^2} - \frac{1}{r}\right)\sum_{n=0}\left(-\frac{n\pi}{L}\right)\tilde{A}(n,t)\sin\frac{n\pi z}{L} - C_{44}\frac{2n\pi}{L^2}\sum_{\xi_i}\frac{\sum_{n=1}\tilde{U}_{\theta d}(\xi_i,n,t)\sin\dfrac{n\pi z}{L}}{F(\xi_i)}C_1(\xi_i r). \tag{34}$$

3. Examples and discussions

In the practical engineering applications, the general form of torsion impact load can be considered as

$$A(z,t) = \tau_0 z\mathrm{e}^{-\beta t}, \quad t \geqslant 0, \tag{35}$$

where β represents the decaying factor. When $\beta \neq 0$, the load function $A(z,t)$ expresses an exponential decaying torsion impact load. When $\beta = 0$, the load function $A(z,t)$ expresses a sudden torsion impact load.

The initial condition before the loading is considered as

$$U_\theta(r,z,0) = 0, \quad \frac{\partial U_\theta(r,z,0)}{\partial t} = 0\,. \tag{36}$$

Substituting Eqs. (35) and (36) into Eqs. (33), the displacement field and the correspondent dynamic shear stress in the structure are, respectively, expressed as

$$U_\theta(r,z,t) = \frac{\tau_0 a^2\mathrm{e}^{-\beta t}}{2C_{66}}\left(\frac{r}{b^2} - \frac{1}{r}\right)\left\{\frac{L}{2} + \frac{2}{\pi^2}\sum_{n=1}^{\infty} n^2[(-1)^n - 1]\cos\frac{n\pi z}{L}\right\}$$

$$+ \sum_{\xi_i}\frac{\tau_0}{F(\xi_i)}\left\{\frac{L\mathrm{J}_1(\xi_i b)}{C_{66}\pi\xi_i^2 J_a}\left[\frac{-\beta C_\tau\xi_i\sin(\omega_i t) + \omega_i^2\cos\omega_i t + \beta^2\mathrm{e}^{-\beta t}}{\beta^2 + \omega_i^2}\right]\right.$$

$$\left. + \frac{4L\mathrm{J}_1(\xi_i b)}{\pi^3 J_a}\sum_{n=1}^{\infty}\frac{1}{n^2}[(-1)^n - 1]\left[\frac{\mathrm{e}^{-\beta t}}{C_{66}\xi_i^2} - \frac{1}{\rho X}\right]\cos\frac{n\pi z}{L}\right\}C_1(\xi_i r), \tag{37}$$

$$\tau_{r\theta}(r,z,t) = \frac{\tau_0 a^2 e^{-\beta t}}{r^2}\left\{\frac{L}{2} + \frac{2}{\pi^2}\sum_{n=1} n^2[(-1)^n - 1]\cos\frac{n\pi z}{L}\right\}$$
$$+ \sum_{\xi_i}\frac{\tau_0}{F(\xi_i)}\left\{\frac{LJ_1(\xi_i b)}{C_{66}\pi\xi_i^2 J_a}\left[\frac{-\beta\omega_i\sin(\omega_i t) + \omega_i^2\cos(\omega_i t) + \beta^2 e^{-\beta t}}{\beta^2 + \omega_i^2}\right]\right.$$
$$\left. + \frac{4LJ_1(\xi_i b)}{\pi^3 J_a}\sum_{n=1}^{\infty}\frac{1}{n^2}[(-1)^n - 1]\left[\frac{1}{C_{66}\xi_i^2} - \frac{1}{\rho X}\frac{\beta\sin(Xt) - X\cos Xt + Xe^{-\beta t}}{\beta^2 + X^2}\right]\cos\frac{n\pi z}{L}\right\}$$
$$\times\left[\xi_i C_0(\xi_i r) - \frac{2}{r}C_1(\xi_i r)\right], \tag{38}$$

$$\tau_{\theta z}(r,z,t) = \frac{\tau_0 a^2 C_{44} e^{-\beta t}}{2C_{66}}\left(\frac{r}{b^2} - \frac{1}{r}\right)\sum_{n=1}^{\infty}\frac{L}{n\pi}[1 + (-1)^{n+1}]\sin\frac{n\pi z}{L}$$
$$- \sum_{\xi_i}\frac{\tau_0}{F(\xi_i)}\frac{4C_{44}J_1(\xi_i b)}{\pi^2 J_a}C_1(\xi_i r)$$
$$\times\left\{\sum_{n=1}^{\infty}\frac{1}{n}[(-1)^n - 1]\left(\frac{1}{C_{66}\xi_i^2} - \frac{1}{\rho X}\frac{\beta\sin(Xt) - X\cos Xt + Xe^{-\beta t}}{X^2}\right)\sin\frac{n\pi z}{L}\right\}, \tag{39}$$

where

$$C_0(\xi_i r) = J_0(\xi_i r)Y_0(\xi_i b) - J_0(\xi_i b)Y_0(\xi_i r). \tag{40}$$

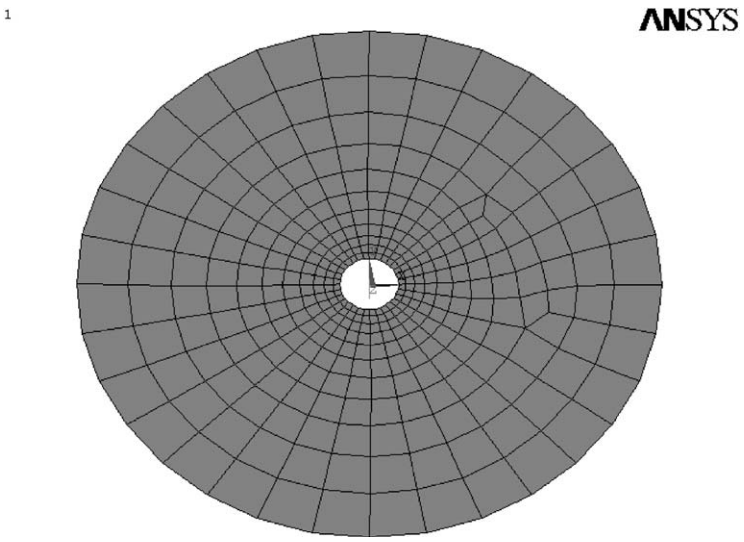

Fig. 2. The finite-element net for the middle plane at $z^* = 0.5$ in the finite length of an orthotropic hollow cylinder under a sudden torsion load for $\beta = 0$. $(b-a)/a = 10$.

In calculating examples, to improve the convergence of these series in the expression of the solution, we consult a particularly useful book 'An introduction to Fourier analysis and generalized functions' in Ref. [11]. Material properties of an orthotropic hollow cylinder in the solutions are considered as: $C_{44} = 80\,\text{GPa}$, $C_{66} = 50\,\text{GPa}$, $\rho = 5000\,\text{kg/m}^3$. The thickness of the two kinds of hollow cylinders are, respectively, $(b-a)/a = 20$ and $(b-a)/a = 2$. In order to make the problem easy to deal with, all the variables are taken in the form of dimensionless quantities such as $T^* = tC_\tau/a$, $R^* = (r-a)/a$, $R1 = (r-a)/(b-a)$, $Z^* = z/L$, $\tau^*_{r\theta} = \tau_{r\theta}/\tau_0$, $\tau^*_{\theta z} = \tau_{\theta z}/\tau_0$, and $U^*_\theta = U_\theta/\tau_0\,(\text{m/Pa})$.

In order to prove further the validity of the analytical method and the solving process, a dynamic finite-element solution for the same example used in the theoretical solution is also achieved by applying the ANSYS finite-element analysis system. In this dynamic equation of the

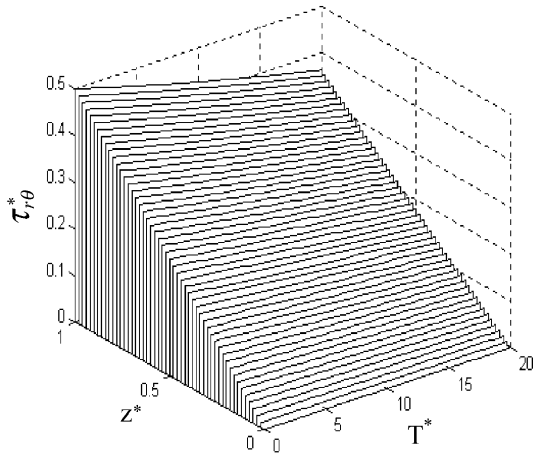

Fig. 3. The responding histories of shear stress in a finite-length orthotropic hollow cylinder under an exponential decaying impact load for $\beta = 500$. $R^* = 0$, $(b-a)/a = 20$, $R^* = (r-a)/a$, $T^* = tC_L/a$, $Z^* = z/L$.

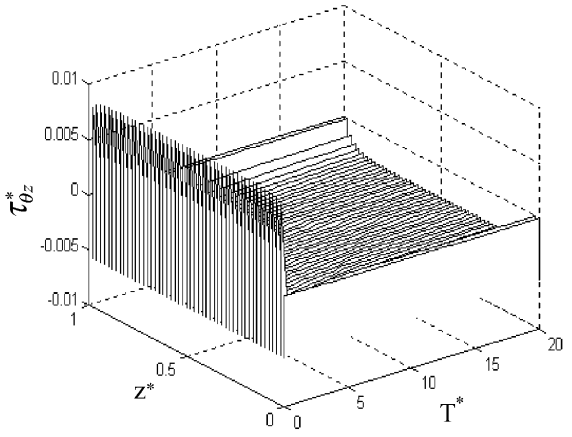

Fig. 4. The responding histories of shear stress in a finite-length orthotropic hollow cylinder under an exponential decaying impact load for $\beta = 500$. $R^* = 0$, $(b-a)/a = 20$, $R^* = (r-a)/a$, $T^* = tC_L/a$, $Z^* = z/L$.

elastic system, applying the Hamilton principle, the dynamic equation of finite element is written as

$$[K]\{d\} + [M]\{\ddot{d}\} = \{F(t)\}, \tag{41}$$

where $[K]$ is the stiff matrix, $[M]$ is the weight matrix, $\{d\}$ is the displacement of the knot point and $\{F(t)\}$ is the dynamic load. In the solving process of the dynamic finite element, applying a direct integral method, the solution of dynamic equation (41) can be obtained in the ANSYS program system. Considering the orthotropic hollow cylinder shown in Fig. 1, the finite-element model and net for the middle plane at $z^* = 0.5$ in the orthotropic hollow cylinder is as shown in

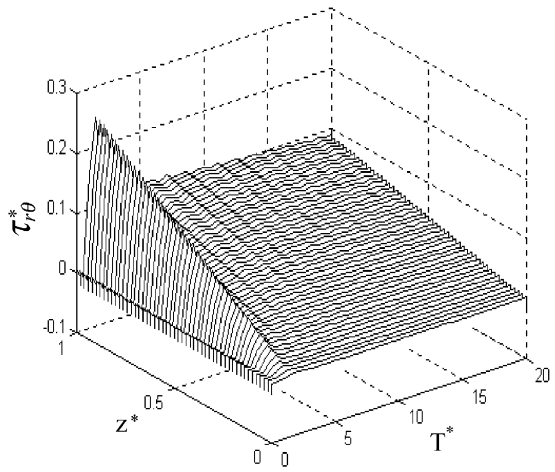

Fig. 5. The responding histories of shear stress in a finite-length orthotropic hollow cylinder under an exponential decaying impact load for $\beta = 500$. $R^* = 1$, $(b-a)/a = 20$, $R^* = (r-a)/a$, $T^* = tC_L/a$, $Z^* = z/L$.

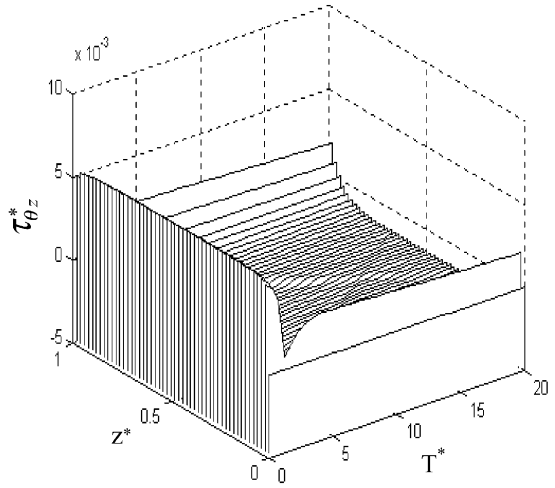

Fig. 6. The responding histories of shear stress in a finite-length orthotropic hollow cylinder under an exponential decaying impact load for $\beta = 500$. $R^* = 1$, $(b-a)/a = 20$, $R^* = (r-a)/a$, $T^* = tC_L/a$, $Z^* = z/L$.

Fig. 2. The geometry size and material property are the same as those in the theoretical solution. Calculating time step $\Delta t = 0.015a/C_\tau$ is taken. Convergence error is less than 0.5%.

The response histories and distributions of dynamic stress and tangential displacement in an orthotropic hollow cylinder with $(b-a)/a = 20$, subjected to an exponential decaying torsion impact load are shown in Figs. 3–6. The response histories and distributions of dynamic stress and tangential displacement in an orthotropic hollow cylinder with $(b-a)/a = 20$, subjected to a sudden torsion load are shown in Figs. 7–12. In order to have a confirmation of the validity of the solution, a special case in computing time $T^* \leqslant 20$ is taken. When the computing time $T^* \leqslant 20$, that is before the wavefront of stress wave arrives at the exterior boundary $r = b$, reflected waves have not been produced so that the reflecting effects of the stress wave in the structure can be avoided.

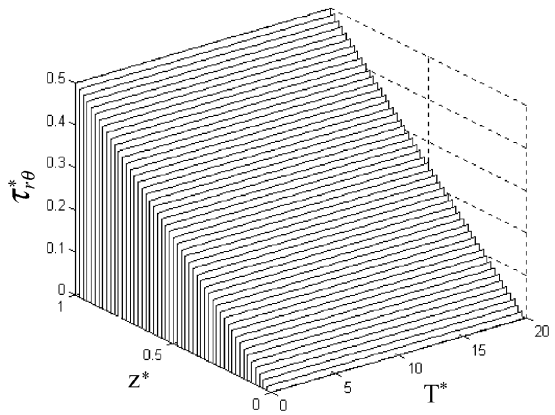

Fig. 7. The responding histories of shear stress in a finite-length orthotropic hollow cylinder under a sudden impact load for $\beta = 0$. $R^* = 0$, $(b-a)/a = 20$, $R^* = (r-a)/a$, $T^* = tC_L/a$, $Z^* = z/L$.

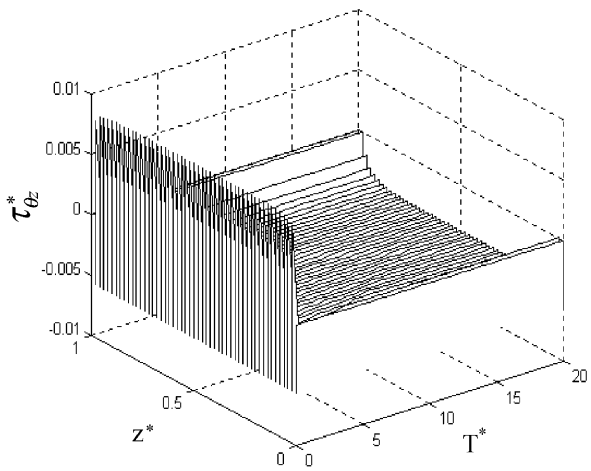

Fig. 8. The responding histories of shear stress in a finite-length orthotropic hollow cylinder under a sudden impact load for $\beta = 0$. $R^* = 0$, $(b-a)/a = 20$, $R^* = (r-a)/a$, $T^* = tC_L/a$, $Z^* = z/L$.

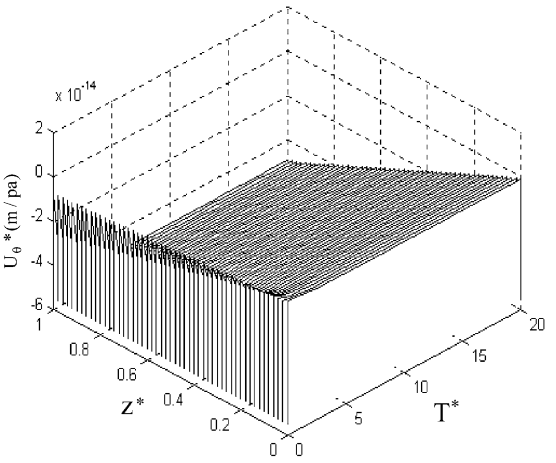

Fig. 9. The responding histories of tangential displacement in a finite-length orthotropic hollow cylinder under a sudden impact load for $\beta = 0$. $R^* = 0$, $(b-a)/a = 20$, $R^* = (r-a)/a$, $T^* = tC_L/a$, $Z^* = z/L$.

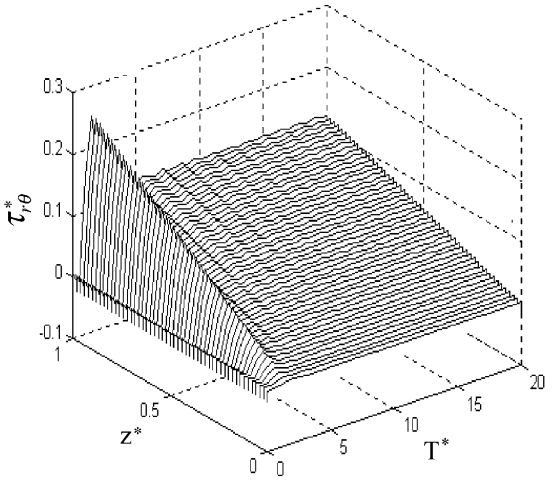

Fig. 10. The responding histories of shear stress in a finite-length orthotropic hollow cylinder under a sudden impact load for $\beta = 0$. $R^* = 1$, $(b-a)/a = 20$, $R^* = (r-a)/a$, $T^* = tC_L/a$, $Z^* = z/L$.

By viewing these figures, the solution is satisfied with the given boundary condition. The dynamic stress $\tau^*_{r\theta}$ at internal surface $R^* = 0$ is not changed with time, and equals the given boundary value $A(z,t)$ shown, respectively, in Figs. 3 and 7. At $z^* = 0$ and $z^* = 1$, which are at the two ends of the finite length of the hollow cylinder, dynamic shear stress $\tau^*_{r\theta}$ is satisfied with the given end condition ($\tau^*_{r\theta} = 0$) shown in Figs. 4, 6, 8 and 11. From Figs. 4–6 and 8–12, we can see that the shear stress and tangential displacement where the wavefront arrives appear in the maximum value and are highly discontinuous. When the wavefront propagates from the point to the external boundary, the stress at the point will gradually decay from the maximum to quasi-static solution at the point.

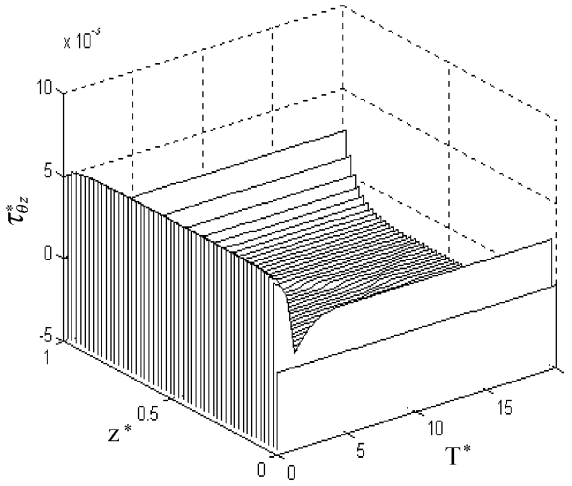

Fig. 11. The responding histories of shear stress in a finite-length orthotropic hollow cylinder under a sudden impact load for $\beta = 0$. $R^* = 1$, $(b-a)/a = 20$, $R^* = (r-a)/a$, $T^* = tC_L/a$, $Z^* = z/L$.

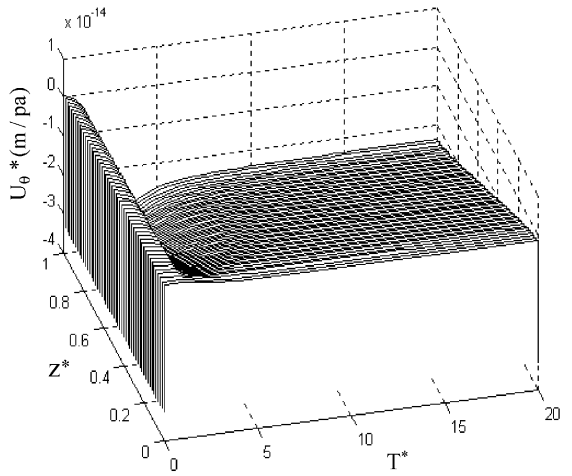

Fig. 12. The responding histories of tangential displacement in a finite-length orthotropic hollow cylinder under a sudden impact load for $\beta = 0$. $R^* = 1$, $(b-a)/a = 20$, $R^* = (r-a)/a$, $T^* = tC_L/a$, $Z^* = z/L$.

Figs. 13–18 represent the responding histories and distributions of shear stress and tangential displacement with time and along the axial direction in an orthotropic hollow cylinder with $(b-a)/a = 2$, under a sudden torsion load. The calculating time is taken as $T^* \leqslant 20$; the reflection effects of wave between the internal and external surfaces have appeared in the responding histories and distributions of stress and displacement in the structure with $(b-a)/a$. As shown in the figures, except the shear stresses at the internal surface and the two free ends, which are satisfied with the given boundary and end conditions, the responding histories and distributions of shear stresses and tangential displacement at the other points of the hollow cylinder appear in dramatical oscillation with time.

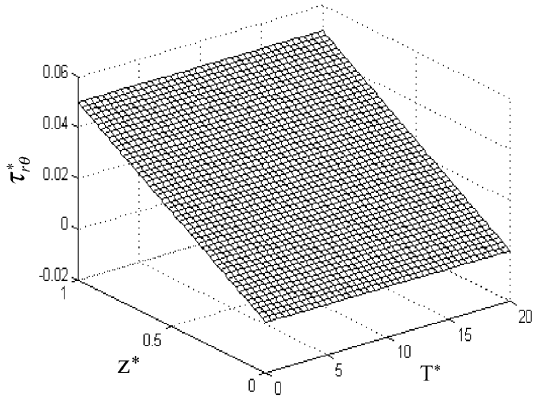

Fig. 13. The responding histories of shear stress in a finite-length orthotropic hollow cylinder under a sudden impact load for $\beta = 0$. $R1 = 0$, $(b-a)/a = 2$, $R1 = (r-a)/(b-a)$, $T^* = tC_L/a$, $Z^* = z/L$.

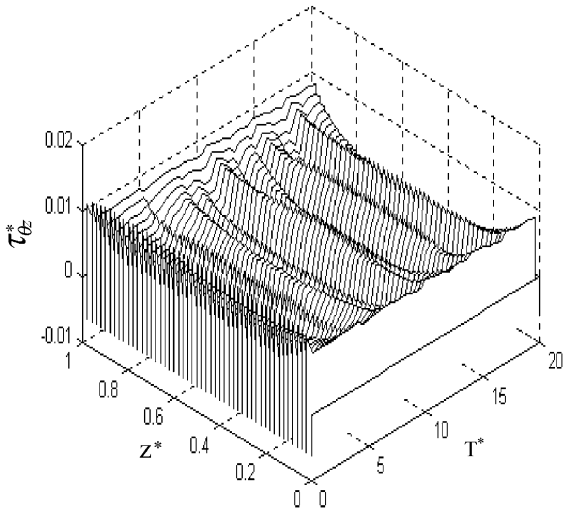

Fig. 14. The responding histories of shear stress in a finite-length orthotropic hollow cylinder under a sudden impact load for $\beta = 0$. $R1 = 0$, $(b-a)/a = 2$, $R1 = (r-a)/(b-a)$, $T^* = tC_L/a$, $Z^* = z/L$.

Figs. 19 and 20 express, respectively, the analytical solution and finite-element solution of the responding histories and distributions of shear stress in the middle plane ($z^* = 0.5$) of the finite-length hollow cylinder with thick $(b-a)/a = 20$, under a sudden torsion load. The features of the stress waves propagating in the hollow cylinder along the radial direction are clearly shown in these figures. The responses of shear stress at which the wavefront of stress wave has not arrived equals zero. The responses of shear stress at which the wavefront arrives appear in the maximum value and strong discontinuous effects. The propagation of the wavefront decays and the dynamic stress approaches the static stress at the same point when time is large and the effect of reflected dose not appear. Comparing the theoretical solution with finite-element solution, it can be found that the two kinds of results obtained by making use of two different solving methods are suitably

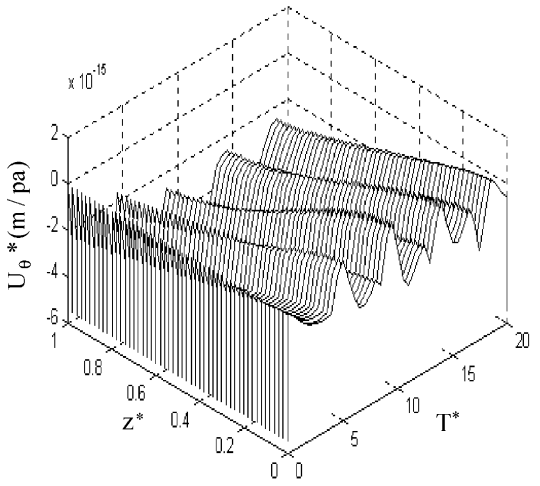

Fig. 15. The responding histories of tangential displacement in a finite-length orthotropic hollow cylinder under a sudden impact load for $\beta = 0$. $R1 = 0$, $(b - a)/a = 2$, $R1 = (r - a)/(b - a)$, $T^* = tC_L/a$, $Z^* = z/L$.

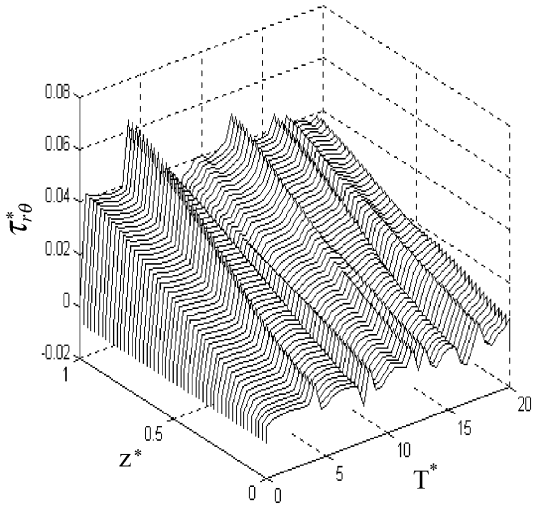

Fig. 16. The responding histories of shear stress in a finite-length orthotropic hollow cylinder under a sudden impact load for $\beta = 0$. $R1 = 0$, $(b - a)/a = 2$, $R1 = (r - a)/(b - a)$, $T^* = tC_L/a$, $Z^* = z/L$.

approached. Therefore, it is further concluded that the method and computing process of the theoretical solution are effective and accurate.

From the above, one concludes that the present closed solution of the finite length of the orthotropic hollow cylinder subjected to torsion impact appears in the features of the stress waves propagating, and is valid theoretically and may be used as a reference to solve other dynamic problems.

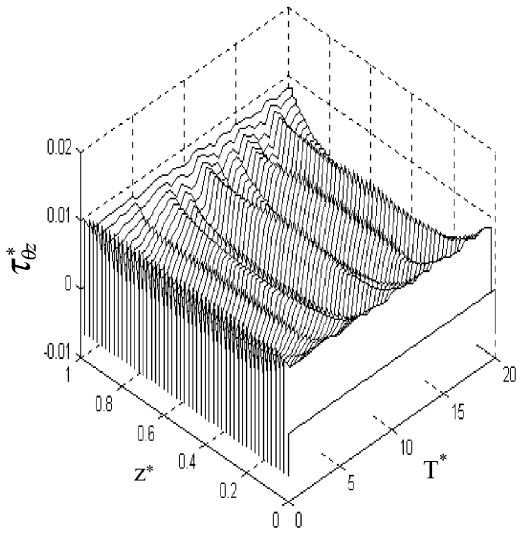

Fig. 17. The responding histories of shear stress in a finite-length orthotropic hollow cylinder under a sudden impact load for $\beta = 0$. $R1 = 0$, $(b-a)/a = 2$, $R1 = (r-a)/(b-a)$, $T^* = tC_L/a$, $Z^* = z/L$.

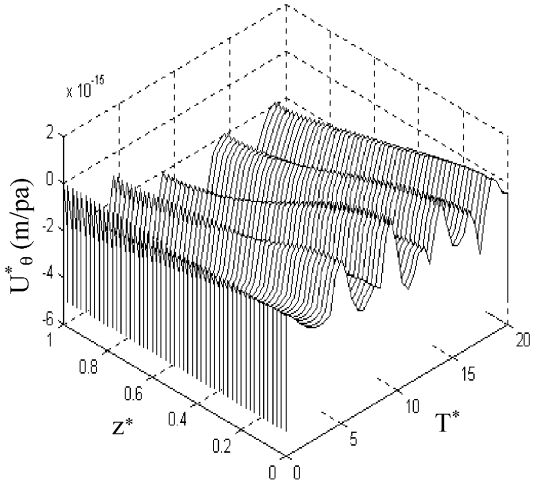

Fig. 18. The responding histories of tangential displacement in a finite-length orthotropic hollow cylinder under a sudden impact load for $\beta = 0$. $R1 = 0$, $(b-a)/a = 2$, $R1 = (r-a)/(b-a)$, $T^* = tC_L/a$, $Z^* = z/L$.

Acknowledgements

This project was supported by the National Natural Science Foundation of China (19972041). The authors thank the referees for their valuable comments.

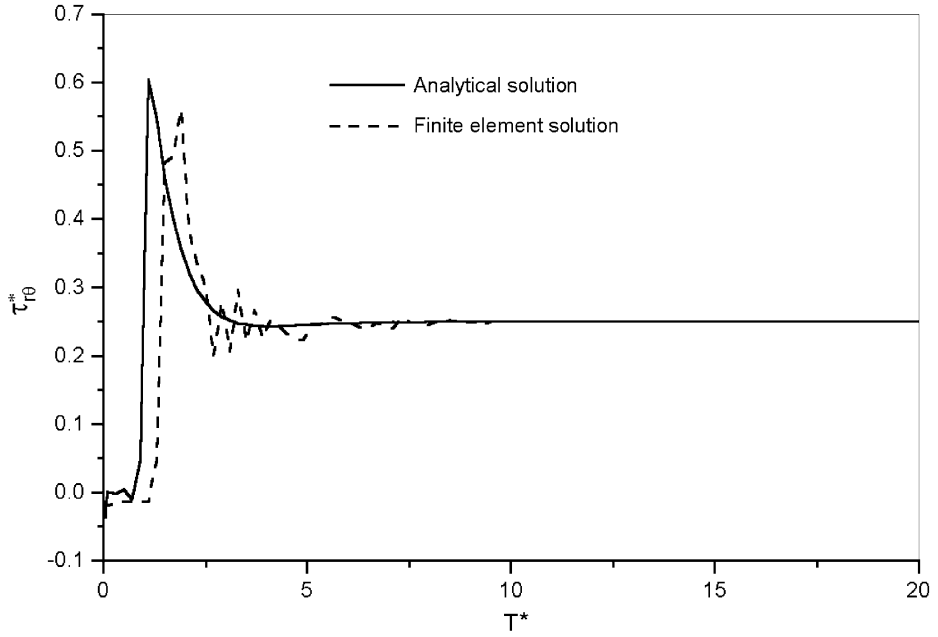

Fig. 19. The response histories of shear stress in the $r-\theta$ plane at $z^*=0.5$ in a finite-length orthotropic hollow cylinder under a sudden torsion load for $\beta=0$. $(b-a)/a=20$, $R^*=1$, $R^*=(r-a)/a$, $T^*=tC_L/a$, $\tau^*_{r\theta}=\tau_{r\theta}/\tau_0$.

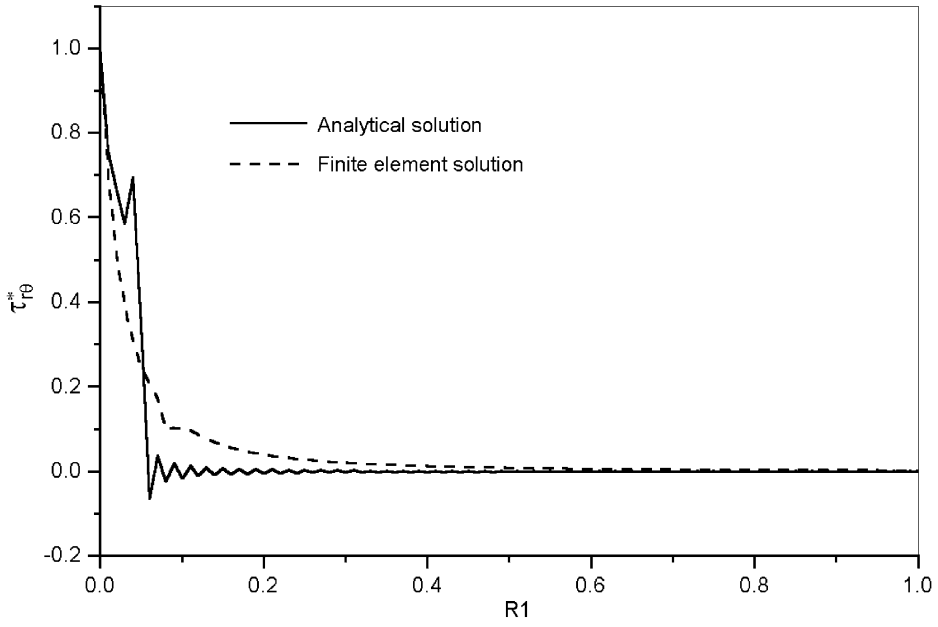

Fig. 20. The distribution of shear stress in the $r-\theta$ plane at $z^*=0.5$ in a finite-length orthotropic hollow cylinder under a sudden torsion load for $\beta=0$. $(b-a)/a=20$, $T^*=1$, $T^*=tC_L/a$, $R1=(r-a)/(b-a)$, $\tau^*_{r\theta}=\tau_{r\theta}/\tau_0$.

Appendix A. Nomenclature

u_θ	tangential displacement
ε_{ij} and σ_{ij}	strains and stresses
$\tau_{r\theta}$	shear stress in the $r\theta$ plane
$\tau_{\theta z}$	shear stress in the θz plane
$u_{\theta s}$	quasi-static displacement solution
$u_{\theta d}$	displacement solution of the non-homogeneous dynamic equation
c_{ij}	elastic coefficients of the material
C_{44}	shear module in the θz co-ordinate plan
C_{66}	shear module in the $r\theta$ co-ordinate plan
ρ and t	density of material and time variable
a, b and L	internal radii, external radii and length of hollow cylinder
$C_\tau = \sqrt{C_{66}/\rho}$	elastic wave speed
$a(z, t)$	torsion impact load function
$J_1(\xi_i r)$ and $Y_1(\xi_i r)$	first order Bessel function of the first and second kinds
$J_0(\xi_i r)$ and $Y_0(\xi_i r)$	zero order Bessel function of the first and second kinds
$\xi_i\ (i = 1, 2, 3, \ldots)$	positive eigenroots

Non-dimensional quantities

$T^* = tC_\tau/a$, $R^* = (r-a)/a$, $R1 = (r-a)/(b-a)$, $Z^* = z/L$, $\tau^*_{r\theta} = \tau_{r\theta}/\tau_0$, $\tau^*_{\theta z} = \tau_{\theta z}/\tau_0$, $U^*_\theta = U_\theta/\tau_0(m/Pa)$.

References

[1] H. Cho, G.A. Kardomateas, C.S. Valle, Elasticodynamic solution for the thermal shock stress in an orthotropic thick cylindrical shell, American Society of Mechanical Engineers, Journal of Applied Mechanics 65 (1) (1998) 184–193.
[2] Wang Xi, An elastodynamic solution for an anisotropic hollow sphere, International Journal of Solid Structures 31(7) (1994) 903–911.
[3] W.E. Baker, Axisymmetric models of vibration of thin spherical shell, Journal of the Acoustical Society of America 33 (1961) 1749–1758.
[4] W.E. Baker, W.C.L. Hu, T.R. Jackson, Elastic response of the thin spherical shell to axisymmetric blast loading, Journal of Applied Mechanics, American Society of Mechanical Engineers 33 (1966) 800–806.
[5] Y.H. Pao, A.N. Ceranoglu, Determination of transient response of thick-walled spherical shell by the Ray theory, Journal of Applied Mechanics, American Society of Mechanical Engineers 45 (1978) 114–122.
[6] J.L. Rose, S.C. Chou, P.C. Chou, Vibration analysis of thick-walled spheres and cylinders, Journal of the Acoustical Society of America 53 (1973) 771–776.
[7] M. Rahman, Some fundamental axisymmetric singular solution of elastodynamics, Quarterly Journal on Mechanics Application 48 (Part 3) (1995) 146–154.
[8] Jin O. Kim, Torsional stress waves in a circular cylinder with a modulated surface, Journal of Applied Mechanics, American Society of Mechanical Engineers 58 (1991) 710–715.
[9] G. Cinell, Dynamic vibrations and stress in the elastic cylinders and spheres, Journal of Applied Mechanics, American Society of Mechanical Engineers 33 (1966) 825–830.
[10] G. Cinell, An extension of the finite Hankel transform and applications, International Journal of Engineering Science 3 (1965) 539–559.
[11] M.J. Lighthill, An Introduction to Fourier Analysis and Generalized Function, Cambridge University Press, Cambridge, 1958.